

c-Jun NH₂-Terminal Kinase 1/2 and Endoplasmic Reticulum Stress as Interdependent and Reciprocal Causation in Diabetic Embryopathy

Xuezheng Li,^{1,3} Cheng Xu,¹ and Peixin Yang^{1,2}

Embryos exposed to high glucose exhibit aberrant maturational and cytoarchitectural cellular changes, implicating cellular organelle stress in diabetic embryopathy. c-Jun-N-terminal kinase 1/2 (JNK1/2) activation is a causal event in maternal diabetes-induced neural tube defects (NTD). However, the relationship between JNK1/2 activation and endoplasmic reticulum (ER) stress in diabetic embryopathy has never been explored. We found that maternal diabetes significantly increased ER stress markers and induced swollen/enlarged ER lumens in embryonic neuroepithelial cells during neurulation. Deletion of either *jnk1* or *jnk2* gene diminished hyperglycemia-induced ER stress markers and ER chaperone gene expression. In embryos cultured under high-glucose conditions (20 mmol/L), the use of 4-phenylbutyric acid (4-PBA), an ER chemical chaperone, diminished ER stress markers and abolished the activation of JNK1/2 and its downstream transcription factors, caspase 3 and caspase 8, and Sox1 neural progenitor apoptosis. Consequently, both 1 and 2 mmol/L 4-PBA significantly ameliorated high glucose-induced NTD. We conclude that hyperglycemia induces ER stress, which is responsible for the proapoptotic JNK1/2 pathway activation, apoptosis, and NTD induction. Suppressing JNK1/2 activation by either *jnk1* or *jnk2* gene deletion prevents ER stress. Thus, our study reveals a reciprocal causation of ER stress and JNK1/2 in mediating the teratogenicity of maternal diabetes. *Diabetes* 62:599–608, 2013

Pre-existing maternal diabetes significantly induces congenital malformations, such as neural tube defects (NTD) and cardiovascular defects (1,2). Ample experimental evidence provides support that hyperglycemia-induced oxidative stress and apoptosis in target tissues, such as the developing neural tube and the embryonic vasculature, are responsible for the induction of embryonic malformations (3–6). Both transcription (7,8) and nontranscription mechanisms (9,10) are proposed in diabetic embryopathy. However, the cellular events downstream from maternal diabetes leading to apoptosis are still murky. A previous ultracellular study using electronic microscopy (EM) has demonstrated aberrant maturational and cytoarchitectural changes associated with malformations in cultured embryos exposed to high

glucose (11), implicating that cellular organelle stress may be involved in the induction of diabetic embryopathy. Endoplasmic reticulum (ER) stress has recently emerged as a key factor in the pathogenesis of several diabetes complications. Diabetic embryopathy is a severe complication of poorly controlled maternal diabetes in pregnancy. It thus prompts us to examine the role of ER stress in diabetic embryopathy.

The ER is a critical organelle responsible for newly synthesized proteins to be properly folded and modified into their correct three-dimensional structures. This ER function is carried out by a pool of ER-resident molecular chaperone proteins, such as binding immunoglobulin protein (BiP) and calnexin. Accumulation of misfolded and/or aggregated proteins perturbs ER function, resulting in ER stress and the induction of cell apoptosis (12). ER stress activates the unfolded protein response (UPR), which increases the expression of ER chaperones and suppresses new protein synthesis (13). Elevated levels of ER chaperones serve as indices of ER stress. The UPR is triggered by the activation of kinases inositol-requiring protein-1 α (IRE1 α) (14) and protein kinase RNA-like ER kinase (PERK) (15). Activated IRE1 α splices X-box binding protein (XBP1) mRNA and thus converts XBP1 into a potent transcriptional activator that induces many UPR-responsive genes (16). Prolonged activation of IRE1 α and subsequently enhanced expression of C/EBP-homologous protein (CHOP) mediate apoptosis during ER stress (12). PERK increases the expression of proapoptotic CHOP through phosphorylation of eukaryotic initiation factor 2 α (eIF2 α) (17). Because hyperglycemia-induced apoptosis in target tissues causes embryonic malformations (18–20), we propose that ER stress-induced apoptosis plays a critical role in the induction of diabetic embryopathy.

The proapoptotic cellular stress kinase c-Jun-N-terminal kinase 1/2 (JNK1/2) is activated in embryos exposed to maternal hyperglycemia and mediates the proapoptotic effects of hyperglycemia (6). We have previously demonstrated using JNK2 knockout mice that targeted deletion of *jnk2* gene significantly ameliorates hyperglycemia-induced neural tube defects (NTD) (21), supporting the causative role of JNK2 activation in diabetic embryopathy. ER stress induced by accumulation of misfolded proteins in the ER luminal compartment also activates JNK1/2 (22). Specifically, the protein kinase IRE1 α couples the ER stress to JNK1/2 activation (22). However, it is unknown whether JNK1/2 activation is sufficient to lead to ER stress. Using our unique mouse model of diabetic embryopathy, which is associated with both JNK1/2 activation and ER stress, we will test the reciprocal relationship between ER stress and JNK1/2 activation in the context of hyperglycemia-induced NTD.

In the current study, using two complementary models, the in vivo maternal diabetes-induced embryopathy model

From the ¹Department of Obstetrics, Gynecology and Reproductive Sciences, University of Maryland School of Medicine, Baltimore, Maryland; the ²Department of Biochemistry and Molecular Biology, University of Maryland School of Medicine, Baltimore, Maryland; and the ³Department of Pharmacy, Affiliated Hospital of Yanbian University, Yanji, Jilin Province, China. Corresponding author: Peixin Yang, pyang@upi.umaryland.edu. Received 6 January 2012 and accepted 18 July 2012.

DOI: 10.2337/db12-0026

This article contains Supplementary Data online at <http://diabetes.diabetesjournals.org/lookup/suppl/doi:10.2337/db12-0026/-/DC1>.

© 2013 by the American Diabetes Association. Readers may use this article as long as the work is properly cited, the use is educational and not for profit, and the work is not altered. See <http://creativecommons.org/licenses/by-nc-nd/3.0/> for details.

and the *in vitro* whole-embryo culture high glucose-induced embryopathy model, we found that ER stress and its associated UPR were robustly present in embryos exposed to hyperglycemia, and treatment with the chemical chaperone 4-phenylbutyric acid (4-PBA), ameliorated ER stress and apoptosis and thus prevented high glucose-induced NTD. Suppressing JNK1/2 activation via *jnk1* or *jnk2* gene deletion abolished hyperglycemia-induced ER stress. Thus, JNK1/2 activation and ER stress are both interdependent and causative events in diabetic embryopathy.

RESEARCH DESIGN AND METHODS

Animals and reagents. C57BL/6J mice, JNK1 heterozygous (*jnk1*^{+/-}), and JNK2 knockout (JNK2KO) mice in C57BL/6J background were purchased from The Jackson Laboratory (Bar Harbor, ME). Streptozotocin (STZ) from Sigma-Aldrich (St. Louis, MO) was dissolved in sterile 0.1 mol/L citrate buffer (pH 4.5). Sustained-release insulin pellets were purchased from Linplint (Linshin, Canada). Plasma insulin levels were assessed by the Rat/Mouse Insulin ELISA kit (Millipore, Billerica, MA; catalog number EZRM-13 K).

Mouse models of diabetic embryopathy. The procedures for animal use were approved by the Institutional Animal Care and Use Committee. For decades, we (21,23,24) and others (7,25–27) have used an internationally accepted rodent model of STZ-induced diabetes in research of diabetic embryopathy. Ten-week old female wild-type (WT), JNK2KO mice, and *jnk1*^{+/-} mice were intravenously injected daily with 75 mg/kg STZ over 2 days to induce diabetes. Blood glucose levels were monitored daily by tail vein puncture and using the FreeStyle Blood Glucose Monitoring System (TheraSense; Abbot, Alameda, CA).

Diabetes was defined as 12-h fasting blood glucose levels ≥ 250 mg/dL, which normally occurred at 3–5 days after STZ injections. Based on a published report (28), male and female mice were paired at 3:00 P.M., and day 0.5 (E0.5) of pregnancy was established by the presence of the vaginal plug in the next morning (8:00 A.M.). On day 5.5 of pregnancy (E5.5), insulin pellets were removed to permit frank hyperglycemia (>250 mg/dL glucose level), so that the developing embryos would be exposed to a hyperglycemic environment during the critical period of closure of the neural tube (neurulation) (E8.0–10.5). Therefore, our mouse model of diabetic embryopathy specifically impacts neurulation and the period of induction of NTD. Based on our extensive studies (18,21,29–31), insulin treatment from E0.5–5.5 is essential for successful embryonic implantation and thus prevents early embryonic lethality (resorption) caused by hyperglycemic exposure at early embryonic stages (\leq E5.5). WT, nondiabetic female mice with vehicle injections and sham operation of insulin pellet implants served as nondiabetic controls. On E8.75 (2:00 P.M. at E8.5), mice were killed, and conceptuses were dissected out of the uteri for analysis. Data on NTD incidences from *jnk2* gene-deleted embryos were not collected, because they have been published elsewhere (21). We have extensively characterized our models in the C57BL/6J background by including surgical (anesthesia) controls and insulin-treated diabetic controls (6,21). The half-life of STZ is only 30 min, and STZ was injected 1 to 2 weeks before pregnancies were established. No residue of toxic effect of STZ on embryonic development in our model was observed in diabetic mice with continuous insulin treatment (6). In our studies, sham operation simulating removal of insulin pellets does not increase the incidence of NTD in nondiabetic mice (6). Consistent with our findings, two independent publications from other groups demonstrate the same finding in the C57BL/6J strain that maternal hyperglycemia induces $>22\%$ NTD (26,27).

Western blotting. Western blotting was performed as previously described (21). Briefly, E8.75 embryos from different experimental groups were sonicated in 80 μ L ice-cold lysis buffer (20 mmol/L tris[hydroxymethyl]aminomethane-HCl [pH 7.5], 150 mmol/L NaCl, 1 mmol/L ethylenediaminetetraacetic acid, 10 mmol/L NaF, 2 mmol/L Na-orthovanadate, 1 mmol/L phenylmethylsulfonyl fluoride, and 1% Triton X-100) containing a protease inhibitor cocktail (Sigma-Aldrich). Equal amounts of protein and the Precision Plus Protein Standards (Bio-Rad) were resolved by SDS-PAGE gels (12% gel for caspase 3 and 8 and 10% gel for all other proteins) and transferred onto Immobilon-P or Immobilon-P^{SQ} (for cleaved caspase) membranes (Millipore). To prevent nonspecific bindings, all membranes were incubated with 5% nonfat milk in PBS (pH 7.0) for 45 min and then were incubated for 18 h at 4°C with the following primary antibodies at 1:1,000 to 1:2,000 dilutions in 5% nonfat milk: BiP, calnexin, phosphorylated (p-)eIF2 α , p-PERK, CHOP, p-JNK1/2, JNK2, JNK1, p-Elk-1 (Ser383), p-c-Jun (Ser63), p-activating transcription factor (ATF) 2 (Thr71), and p-Foxo3a (Thr32) (Cell Signaling Technology, Beverly, MA); anticaspase 3 (Chemicon International, Billerica, MA); and rat anticaspase 8 (mouse specific) (Alexis Biochemicals, San Diego, CA), which detects both procaspase 8 and cleaved

caspase 8. Membranes were exposed to goat anti-rabbit or anti-mouse (Jackson ImmunoResearch Laboratories, West Grove, PA) secondary antibodies. To ensure that equivalent amounts of protein were loaded among samples, membranes were stripped and probed with a mouse antibody against β -actin (Abcam, Cambridge, MA). Signals were detected using an Amersham ECL Advance Detection Kit (GE Healthcare, Piscataway, NJ) or a Supersignal West Pico Chemiluminescent Substrate (Thermo Scientific), and chemiluminescence emitted from the bands was directly captured using a UVP Bioimage EC3 system (UVP, Upland, CA). Densitometric analysis of chemiluminescence signals was performed by VisionWorks LS software (UVP). All experiments were repeated three times with the use of independently prepared tissue lysates.

Detection of XBPI mRNA splicing. mRNA was reverse-transcribed to cDNA, which was used for PCR. The PCR primers were: forward, 5'-AAACA GAGTAGCAGCGCAGACTGC-3' and reverse, 5'-TCCTTCTGGGTAGACCTC TGGGAG-3'. If no XBPI mRNA splicing occurred, one band at 205 bp was produced. Two bands, 205 and 179 bp (a main band), were present in PCR products when XBPI mRNA was spliced.

Whole-embryo culture. The procedure of whole-embryo culture has been previously described elsewhere (21,32). C57BL/6J mice were paired overnight. The next morning was designated embryonic day E0.5 if a vaginal plug was present. Mouse embryos at E8.5 were dissected out of the uteri in PBS (Invitrogen, La Jolla, CA). The parietal yolk sac was removed using a pair of fine forceps, and the visceral yolk sac was left intact. Embryos (four per bottle) were cultured in 4 mL rat serum at 38°C in 30 revolutions/min rotation in the roller bottle system. The culture bottles were gassed with 5% O₂/90% N₂ for the first 24 h and 10% O₂/5% CO₂/85% N₂ for the last 12 h. Embryos were cultured for 12 h (for Western blots) or 36 h (for NTD examination) under 5 mmol/L glucose, a value close to the blood glucose level of nondiabetic mice, or 20 mmol/L glucose, which is equivalent to the blood glucose level of diabetic mice, in the presence or absence of 1 or 2 mmol/L 4-PBA (Sigma-Aldrich). The range of 4-PBA concentrations in cell-culture studies is from 0.5–20 mmol/L (33). We started our whole-embryo culture experiments using 1 and 2 mmol/L 4-PBA and found that 2 mmol 4-PBA completely inhibited high glucose-induced NTD. Therefore, we used 2 mmol/L 4-PBA in our subsequent mechanistic studies. Because treatment of diabetic mice with 4-PBA results in normalization of hyperglycemia (33), *in vivo* 4-PBA administration is not suitable for assessing the direct effect of 4-PBA on maternal diabetes-induced NTD. At the end of 36-h culture, embryos were dissected from the yolk sac and examined under a Leica MZ16F stereomicroscope (Leica Microsystems, Bannockburn, IL) to identify embryonic malformations. Images of embryos were captured by a DFC420 5 MPix digital camera with software (Leica Microsystems). Normal embryos were classified as possessing a completely closed neural tube and no evidence of other malformations. Malformed embryos were classified as showing evidence of failed closure of the neural tube or NTD. The open neural tube structures of NTD embryos were verified by histological sections. Because embryos were only exposed to high glucose during a period of neurulation, NTD were the only structural defects detected in this study. Other malformations such as cardiac abnormalities, which were developed at the late embryonic stage (E15.5), were not within the scope of our study.

EM. Abnormal ER structures were examined by transmission EM, which was done in our EM core facility. Thick sections (1 μ m) were cut and visualized at $\times 100$ and $\times 200$ original magnifications to identify the neuroepithelia of E8.75 embryos. Thin sections (80 nm) of identified neuroepithelia were cut and viewed with an electron microscope (Jeol JEM-1200EX; Jeol, Tokyo, Japan) under high-power resolution (10,000, 12,000, and 25,000) for identification of abnormal ER structures.

Real-time PCR. Total RNA was isolated from E8.75 embryos using an RNeasy Mini Kit (Qiagen, Valencia, CA). Real-time PCR for BiP (*HSPA5*), calnexin, eukaryotic translation initiation factor 2 α kinase 3 (eIF2ak3), eIF2 α ribosome biogenesis regulator homolog (*S. cerevisiae*) (eIF2as1), protein disulfide isomerase family A, member 3 (PDIA3), IRE1 α (*erm1*), and β -actin were performed using ABI TaqMan Gene Expression Assays (Applied Biosystems, Foster City, CA). RNA was reverse transcribed by using the high-capacity cDNA archive kit (Applied Biosystems). Real-time PCR and subsequent calculations were performed by the StepOnePlus Real-time PCR system (Applied Biosystems), which detected the signal emitted from fluorogenic probes during PCR.

Determining numbers of apoptotic cells using transferase-mediated dUTP nick-end labeling (TUNEL) assay. The transferase-mediated dUTP nick-end labeling (TUNEL) assay was performed using the In Situ Cell Death Detection kit (Millipore). Five-micrometer serial coronal sections through the anterior neural tube were fixed with 4% paraformaldehyde in PBS and incubated with TUNEL reaction agents with or without Sox1 immunostaining. TUNEL-positive cells in the neural tube area of each section were counted. Based on the counting of total cell nuclei, the sizes of the neural tube areas of each section were relatively constant. Thus, apoptotic cell numbers were expressed as total

TUNEL-positive cells per neural tube area. TUNEL assays were performed without the observer knowing the experimental groups.

Statistics. Data are presented as means \pm SE. One-way ANOVA was performed using SigmaStat 3.5 software, and a Tukey test was used to estimate the significance. Statistical significance was accepted at $P < 0.05$. Significant difference between groups in malformation incidences was analyzed by χ^2 test.

RESULTS

Maternal diabetes induces ER stress associated with JNK1/2 activation in embryonic tissues during embryonic neurulation. To determine whether maternal diabetes induces ER stress, levels of ER stress markers, BiP, p-PERK, and CHOP were analyzed in E8.75 embryos, a critical time point of neurulation, from nondiabetic and diabetic dams. Levels of BiP, p-PERK, CHOP, and p-JNK1/2 were significantly higher in embryos from diabetic dams than those from nondiabetic dams (Fig. 1A–D). XBP1 mRNA splicing, another ER stress indicator, was analyzed in RNA samples by PCR. Embryos exposed to maternal diabetes exhibited robust splicing manifested with two bands at 205 and 179 bp of the PCR products, whereas embryos from nondiabetic dams showed no XBP1 splicing with only one band (205 bp) of the PCR products (Fig. 1E). Because the main goal of our study was to analyze embryos during neurulation and examine NTD as the ultimate outcome, we determined whether maternal diabetes-induced ER stress mainly occurred in cells of the

developing neuroepithelium. EM was employed to examine the swollen/enlarged ER lumens, which are direct morphological evidence of ER stress. Swollen/enlarged ER lumens were consistently present in neuroepithelial cells in E8.75 embryos exposed to maternal diabetes (Fig. 1F). In contrast, neuroepithelial cells in five embryos from five nondiabetic dams did not show any abnormal ER lumen structure (Fig. 1F). In our model, insulin pellets effectively restored serum insulin levels and euglycemia in diabetic mice (Supplementary Table 1). Because of the relatively short duration of our experiments, diabetes did not significantly affect body weight (Supplementary Table 2).

Deletion of *jnk1* or *jnk2* gene abolishes maternal hyperglycemia-induced ER stress. Because either *jnk1* or *jnk2* gene deletion significantly reduce maternal diabetes-induced JNK1/2 activation (Figs. 2A and 3A), E8.75 *jnk1*^{-/-} embryos from *jnk1*^{+/-} mothers mated with *jnk1*^{+/-} males, and *jnk2*^{-/-} embryos from JNK2KO mice were used to determine the causal role of JNK1/2 activation in ER stress. We found that *jnk1*^{-/-} embryos exposed to hyperglycemia had significantly lower levels of ER stress markers, BiP, p-PERK, CHOP, and p-eIF2 α , than those in WT embryos from the same group of diabetic *jnk1*^{+/-} mothers (Fig. 2B–E). Similarly, *jnk2*^{-/-} embryos from diabetic JNK2KO mice had similar levels of ER stress markers, calnexin, BiP, CHOP, and p-eIF2 α , as those in embryos of nondiabetic WT dams, which were significantly lower than those in embryos from diabetic WT mice (Fig. 3A–D). Moreover,

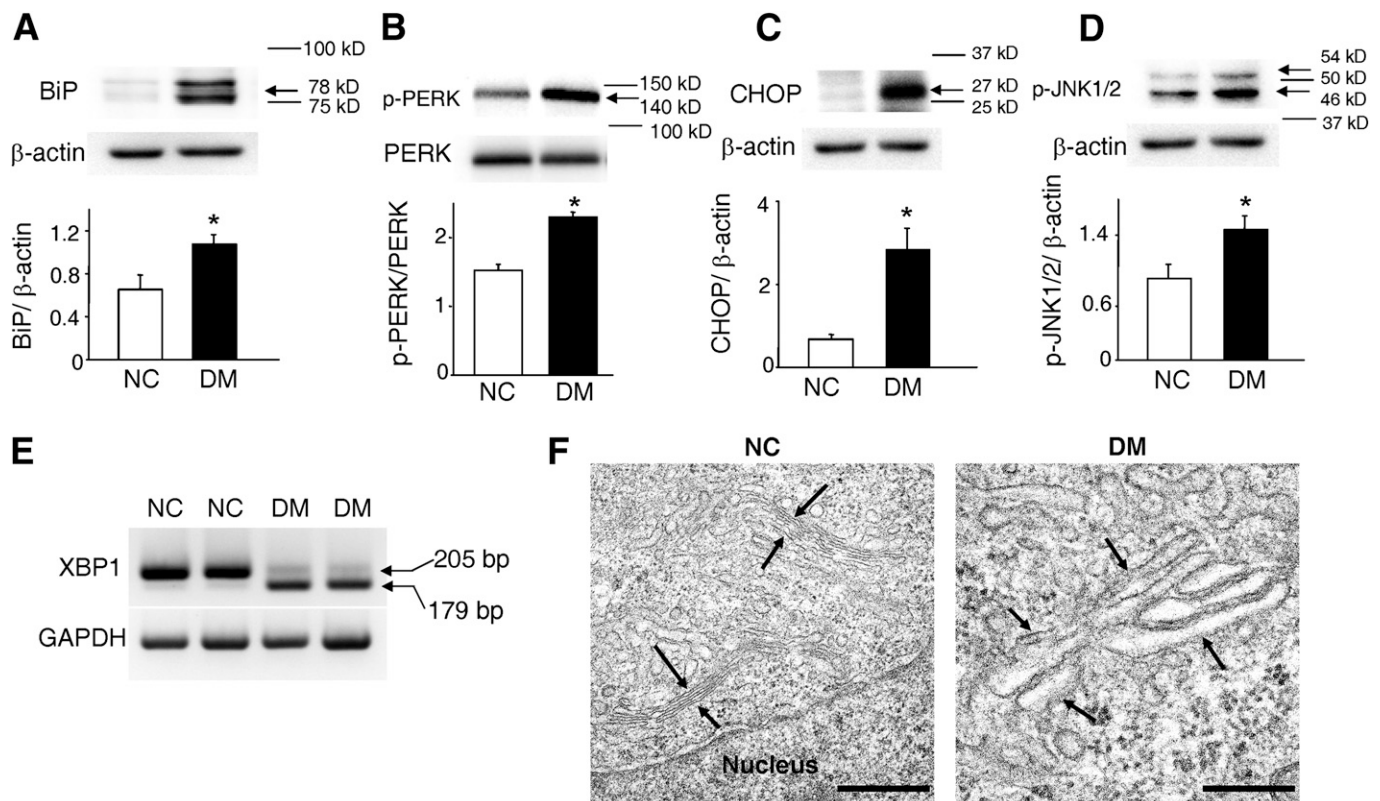


FIG. 1. Maternal diabetes increases the expression of ER stress markers and induces abnormal ER morphology in neuroepithelial cells. Levels of BiP (A), p-PERK (B), CHOP (C), and p-JNK1/2 (D) were determined in E8.75 WT embryos from nondiabetic control (NC) and diabetes mellitus (DM) WT mice. E: XBP1 mRNA splicing was detected by reverse transcription and subsequent PCR. F: ER with swollen/enlarged lumens was observed in neuroepithelial cells of embryos from the DM group but not in those of embryos from the NC group. Black arrows point to the ER. Scale bars, 50 nm. In A–D, arrows point to the actual sizes of the targeted proteins, and adjacent protein markers are indicated. Experiments were repeated three times using samples from different dams in each group. *Significant difference ($P < 0.05$) between the two groups.

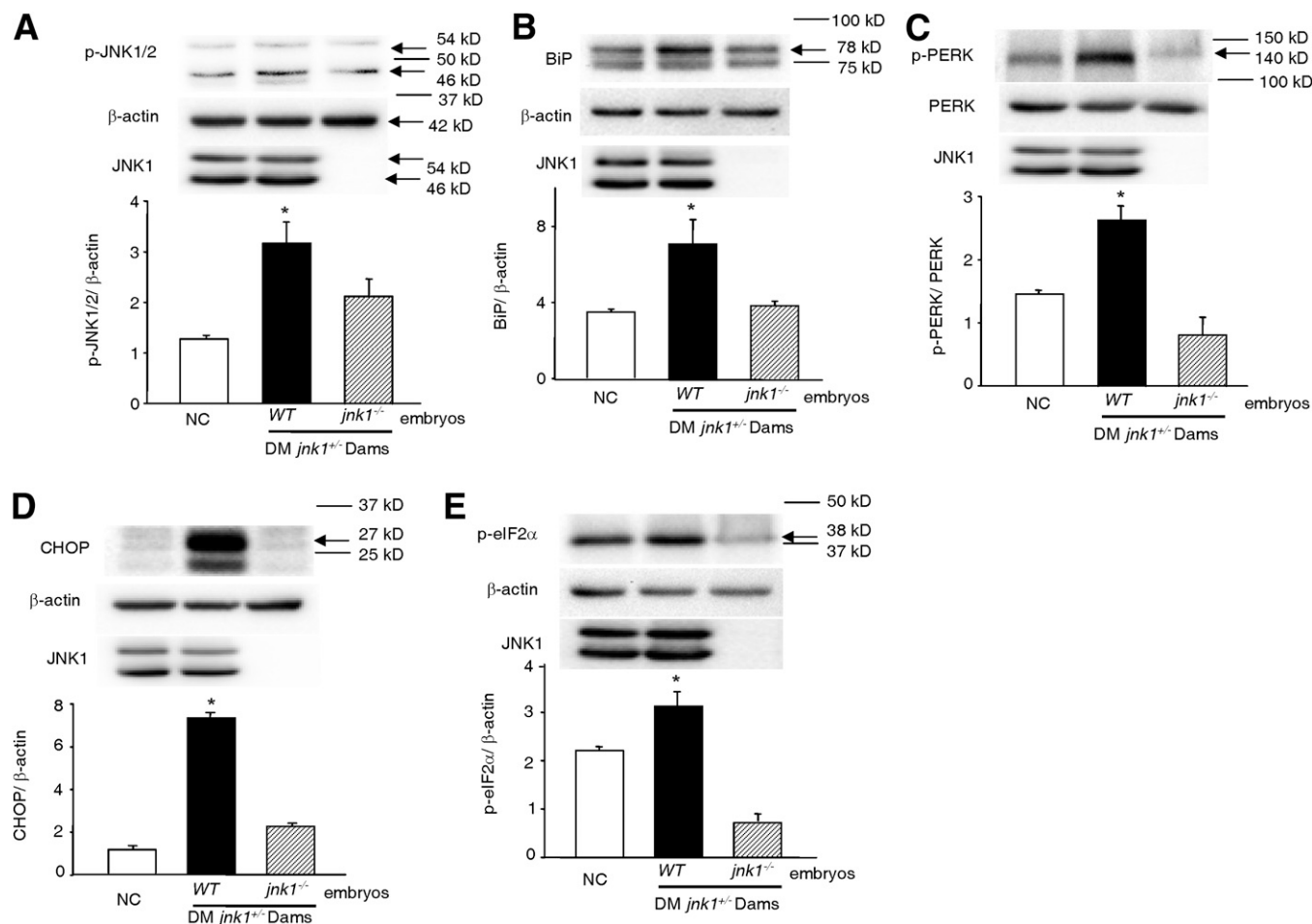


FIG. 2. Deletion of the *jnk1* gene blocks maternal diabetes-induced ER stress. Levels of p-JNK1/2 (A), BiP (B), p-PERK (C), CHOP (D), and p-eIF2α (E) in WT embryos from the nondiabetic control (NC) group and WT embryos and *jnk1*^{-/-} embryos from the same group of diabetic *jnk1*^{+/+} dams (DM-*jnk1*^{+/+}) mated with *jnk1*^{-/-} males. Experiments were repeated three times using samples from different dams in each group. Arrows point to the actual sizes of the targeted proteins, and adjacent protein markers are indicated. *Significant difference ($P < 0.05$) compared with the other two groups.

hyperglycemia-induced XBP1 splicing was diminished in *jnk1*^{-/-} and *jnk2*^{-/-} embryos (Fig. 3E).

***jnk1* or *jnk2* gene deletion reverses maternal hyperglycemia-induced ER chaperone gene expression.**

ER stress increases an array of ER chaperone gene expression. To determine whether JNK1/2 deficiency caused by *jnk1* or *jnk2* gene abrogates maternal diabetes-induced ER chaperone gene expression, mRNA levels of six ER chaperone genes were determined. Maternal diabetes significantly increased the expression of BiP, calnexin, eIF2ak3, eIF2as1, and PDIA3 (Fig. 4A–E). Deletion of either *jnk1* or *jnk2* gene inhibited maternal diabetes-induced expression of BiP, calnexin, eIF2ak3, eIF2as1, and PDIA3 to the levels in the nondiabetic WT group (Fig. 4A–E). Maternal diabetes did not increase IRE1α expression (Fig. 4F). However, either *jnk1* or *jnk2* gene deletion was even able to reduce IRE1α expression (Fig. 4F).

ER chemical chaperone, 4-PBA, effectively blocks hyperglycemia-induced ER stress and resultant NTD.

Because the ER chemical chaperone, 4-PBA, has been shown to block ER stress in other systems, we used 4-PBA to determine whether it could block high glucose-induced ER stress in cultured embryos. Treatment of cultured embryos with 2 mmol/L 4-PBA suppressed high glucose-induced ER stress markers, BiP, CHOP, and p-eIF2α

(Fig. 5A–C). To determine whether ER stress is a causal event leading to NTD, NTD was assessed in cultured embryos with or without 1 mmol/L or 2 mmol/L 4-PBA. The NTD rate in high glucose group was 66.7%, which was significantly higher than those in the 5 mmol/L glucose group (8.0%), the high glucose plus 1 mmol/L 4-PBA group (10.0%), and the high glucose plus 2 mmol/L 4-PBA group (8.3%) (Table 1 and Fig. 5D). The NTD rates in the high glucose plus 1 mmol/L 4-PBA group and the high glucose plus 2 mmol/L 4-PBA group were not significantly different than that in the 5 mmol/L glucose group (Table 1 and Fig. 5D). 4-PBA treatment even reduced NTD rates under 5 mmol/L glucose conditions (Table 1).

Suppressing ER stress by 4-PBA abrogates hyperglycemia-induced JNK1/2 activation and its downstream signaling.

To determine whether 4-PBA treatment suppresses the JNK1/2 pathway, we assessed phosphorylated levels of JNK1/2 and its downstream effectors in cultured embryos treated with 2 mmol/L 4-PBA. 4-PBA treatment completely blocked high glucose-induced phosphorylation of JNK1/2, c-Jun, Elk1, and ATF-2 (Fig. 6A–D). Foxo3a activation depends on its dephosphorylation. High glucose induced Foxo3a dephosphorylation whereas 4-PBA treatment abrogated high glucose-induced Foxo3a dephosphorylation (Fig. 6E).

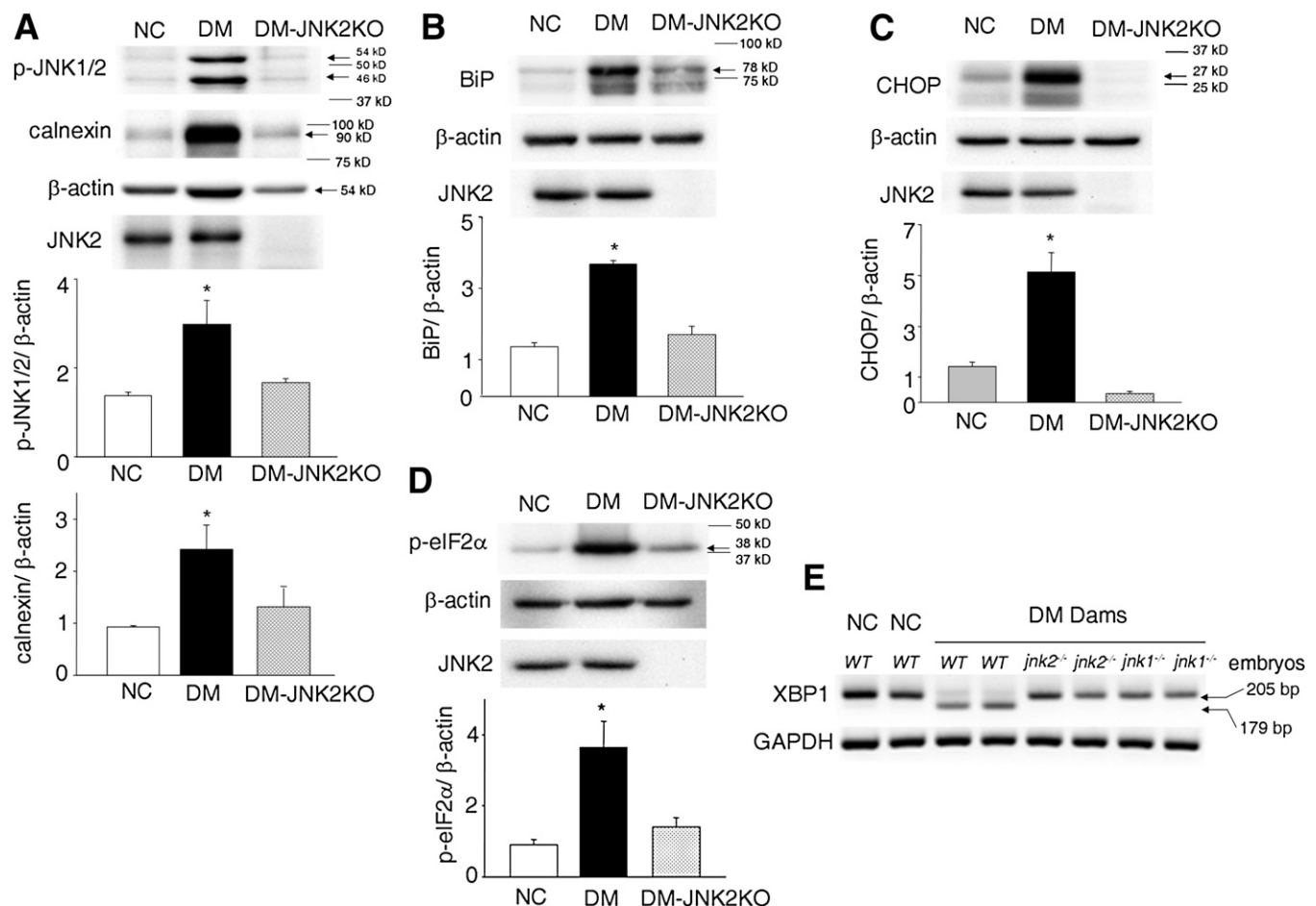


FIG. 3. Deletion of the *jnk2* gene blocks maternal diabetes-induced ER stress. Levels of p-JNK1/2 and calnexin (A), BiP (B), CHOP (C), and p-eIF2 α (D) in WT embryos from the nondiabetic control (NC) group and the diabetes mellitus (DM) group and *jnk2*^{-/-} embryos from diabetic JNK2KO dams (DM-JNK2KO). E: XBP1 mRNA splicing in WT embryos of the NC and DM groups, *jnk2*^{-/-} embryos from diabetic JNK2KO dams, and *jnk1*^{-/-} embryos of diabetic *jnk1*^{+/-} dams mated with *jnk1*^{+/-} males. Experiments were repeated three times using samples from different dams in each group. In A–D, arrows point to the actual sizes of the targeted proteins, and adjacent protein markers are indicated. *Significant difference ($P < 0.05$) compared with the other two groups.

4-PBA abolishes hyperglycemia-induced caspase activation and apoptosis in the neuroepithelium.

Because JNK1/2 activation leads to caspase activation and apoptosis and 4-PBA suppresses JNK1/2 activation, we assessed the effect of 4-PBA on high glucose-induced caspase activation and neuroepithelial cell apoptosis. High glucose induced robust cleavage of caspase 3 and 8 (Fig. 7A). 4-PBA treatment abolished high glucose-induced caspase 3 and 8 cleavage (Fig. 7A). There were significant higher numbers of apoptotic neuroepithelial cells in embryos exposed to high glucose than cells under 5 mmol/L glucose conditions and high glucose plus 4-PBA conditions (Fig. 7B and C). Apoptotic cell numbers in the 5 mmol/L glucose group and the high glucose plus 4-PBA group were comparable (Fig. 7B and C). High glucose-induced apoptotic cells were Sox1 positive neural progenitors (Fig. 7D).

DISCUSSION

We have demonstrated in this series of experiments the reciprocal causative relationship between JNK1/2 activation and ER stress in diabetic embryopathy. Using the ER stress chemical inhibitor, 4-PBA, we determined that high glucose in vitro-induced ER stress mediates the teratogenicity of hyperglycemia through induction of caspase

activation and apoptosis. Deletion of either *jnk1* or *jnk2* gene abrogates maternal diabetes-induced ER chaperone gene expression and consequent ER stress. Therefore, the current study provides mechanistic evidence for the interdependent relationship between JNK1/2 activation and ER stress and for the potential use of ER stress chemical inhibitors, such as 4-PBA, to prevent maternal diabetes-induced embryonic malformations.

Our previous study (11) using EM demonstrated aberrant maturational and cytoarchitectural changes in embryonic cells exposed to high glucose. However, this previous study did not specify which cellular organelle is impacted by high glucose. By assessing total cellular levels of ER stress markers and examining swollen/enlarged ER by EM, the current study clearly reveals that ERs in neuroepithelial cells of the developing neural tube are adversely impacted by maternal diabetes. Three pathways—the IRE1–XBP-1 pathway, the PERK–eIF2 α pathway, and the ATF6–CHOP pathway—collectively constitute the ER-specific UPR (13). The key intermediates of these three pathways can be used as indices of ER stress. Our study demonstrates increased expression of BiP, CHOP, XBP1 splicing, PERK, and eIF2 α phosphorylation, supporting the conclusion that hyperglycemia-induced ER stress activates all three UPR responses. Activation of these UPR pathways, particularly the activation

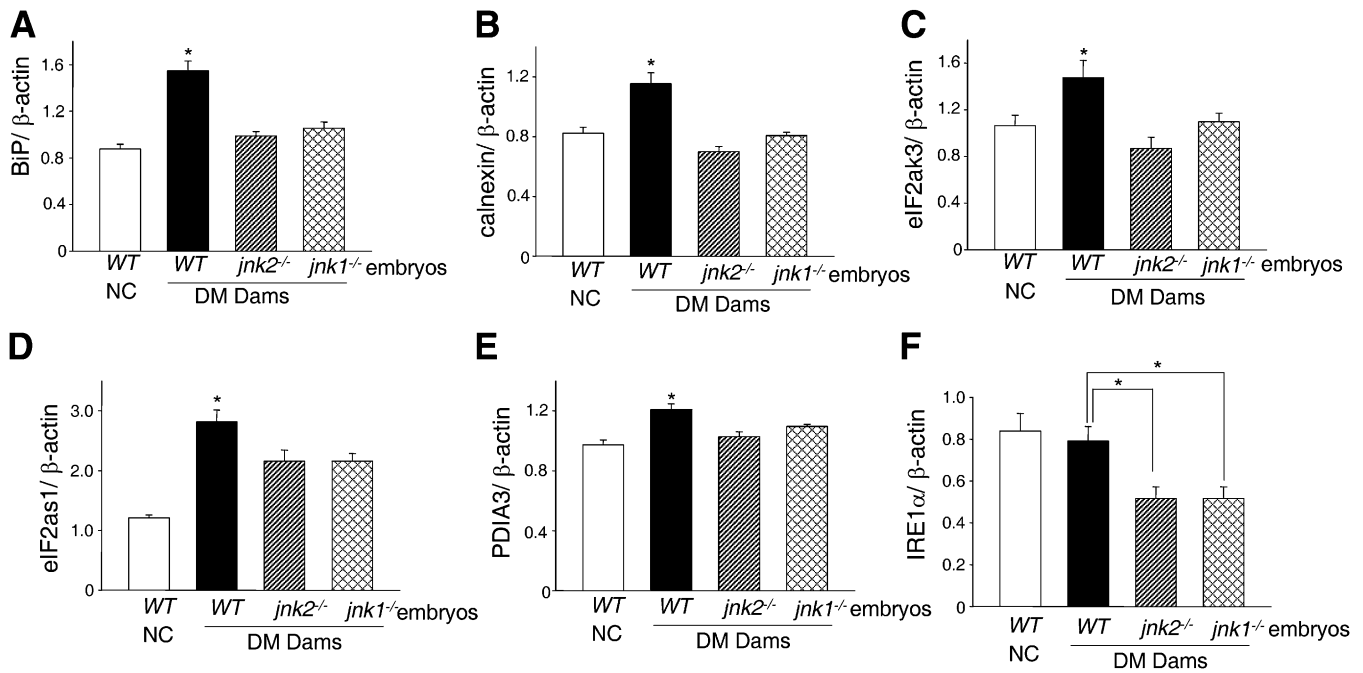


FIG. 4. Targeted deletions of either *jnk1* or *jnk2* gene suppress maternal diabetes-induced ER chaperone gene expression. mRNA levels of BiP (A), calnexin (B), eIF2ak3 (C), eIF2as1 (D), PDIA3 (E), and IRE1α (F) in WT embryos of the nondiabetic control (NC) group and diabetes mellitus (DM) group, *jnk2*^{-/-} embryos from diabetic JNK2KO dams, and *jnk1*^{-/-} embryos of diabetic *jnk1*^{-/-} dams mated with *jnk1*^{-/-} males. Five embryonic samples (*n* = 5) from five different dams of each group were used for real-time PCR. *Significant difference (*P* < 0.05) compared with the other two groups.

of IRE1–XBP1 and CHOP, triggers apoptosis in cells under pathophysiologic conditions (12). These ER stress-induced apoptotic effects are in line with the central apoptotic mechanism in the induction of diabetic

embryopathy (5,6). Indeed, our subsequent studies show that ER stress inhibitor, 4-PBA, blocks apoptosis in cells of the developing neural tube and thus ameliorates high glucose-induced NTD.

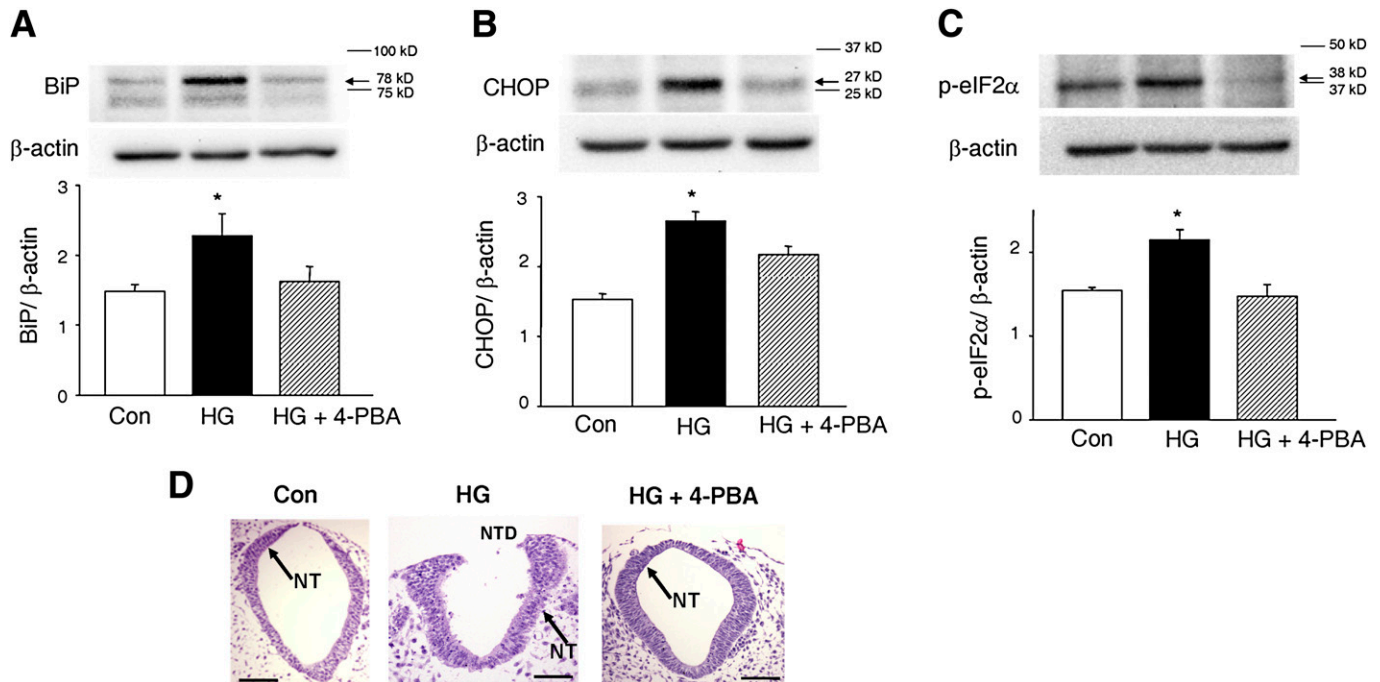


FIG. 5. 4-PBA suppresses high glucose-induced ER stress and NTD formation. Levels of BiP (A), CHOP (B), and p-eIF2α (C) in embryos cultured under 5 mmol/L glucose (control [Con]), 20 mmol/L glucose (high glucose [HG]), and 20 mmol/L glucose plus 2 mmol/L 4-PBA conditions (HG + 4-PBA). Experiments were repeated three times using samples from three independent cultures. D: Representative images of closed neural tubes from the Con group and HG plus 2 mmol/L 4-PBA group and the open neural tube (NT) structure of an NTD embryo from the HG group. Scale bars, 0.5 mm. In A–C, arrows point to the actual sizes of the targeted proteins, and adjacent protein markers are indicated. *Significant difference (*P* < 0.05) compared with the other two groups. (A high-quality color representation of this figure is available in the online issue.)

TABLE 1
High glucose–induced NTD ameliorated by 4-PBA

Experimental groups	Total number of embryos	Total number of malformed embryos	Malformation rates (%)
5 mmol/L glucose + vehicle	25	2 ^a	8.0
5 mmol/L glucose + 2 mmol/L 4-PBA	11	0 ^a	0.0
20 mmol/L glucose + vehicle	24	16 ^b	66.7
20 mmol/L glucose + 1 mmol/L 4-PBA	10	1 ^a	10.0
20 mmol/L glucose + 2 mmol/L 4-PBA	24	2 ^a	8.3

E8.5 embryos were cultured for 36 h, and embryonic NTD was determined. Vehicle is DMSO, which was used to dissolve 4-PBA. Malformation rates are malformed embryos/total number of embryos. ^{a,b}Significant difference between compared groups by χ^2 test ($P < 0.01$).

ER stress induces an array of proapoptotic signaling, which centers on JNK1/2 activation (22,34). We show that both ER stress and JNK1/2 activation are present in diabetic embryopathy. Because 4-PBA has been shown to

attenuate diabetes-induced ER stress (33), in the current study, it was used to test whether amelioration of ER stress can block high glucose–induced proapoptotic signaling. 4-PBA treatment blocks high glucose–induced activation of JNK1/2 and its downstream effectors. These findings strongly support that ER stress is directly linked to or enhances the activation of the proapoptotic JNK1/2 pathway, which leads to caspase activation and apoptosis in diabetic embryopathy.

ER stress also induces oxidative stress (35), which may directly mediate the proapoptotic effect of high glucose on neuroepithelial cells. It is known that oxidative stress increases the expression of Bax (36), a proapoptotic Bcl-2 family member, and suppresses the expression of the antiapoptotic protein, Bcl-2 (37). Oxidative stress plays a central role in the pathogenesis of diabetic embryopathy, which also leads to Bax upregulation and Bcl-2 downregulation (38). Thus, it is possible that high glucose–induced ER stress results in oxidative stress, which, in turn, causes neuroepithelial cell apoptosis via altering the expression of Bcl-2 family members.

Previous studies have demonstrated that high glucose in vitro can rapidly activate JNK1/2 (6,31). In addition, deletion of either *jnk1* or *jnk2* (21) significantly reduces maternal diabetes–induced NTD. These findings, which suggest that JNK1/2 activation may occur before cells undergo ER stress, prompted us to examine whether JNK1/2 activation causes ER stress. JNK1/2 deficiency caused by either *jnk1* or *jnk2* gene deletion abrogates maternal diabetes–increased ER stress markers and ER chaperone gene expression, supporting the conclusion that JNK1/2 activation triggers the UPR response and subsequently induces ER stress.

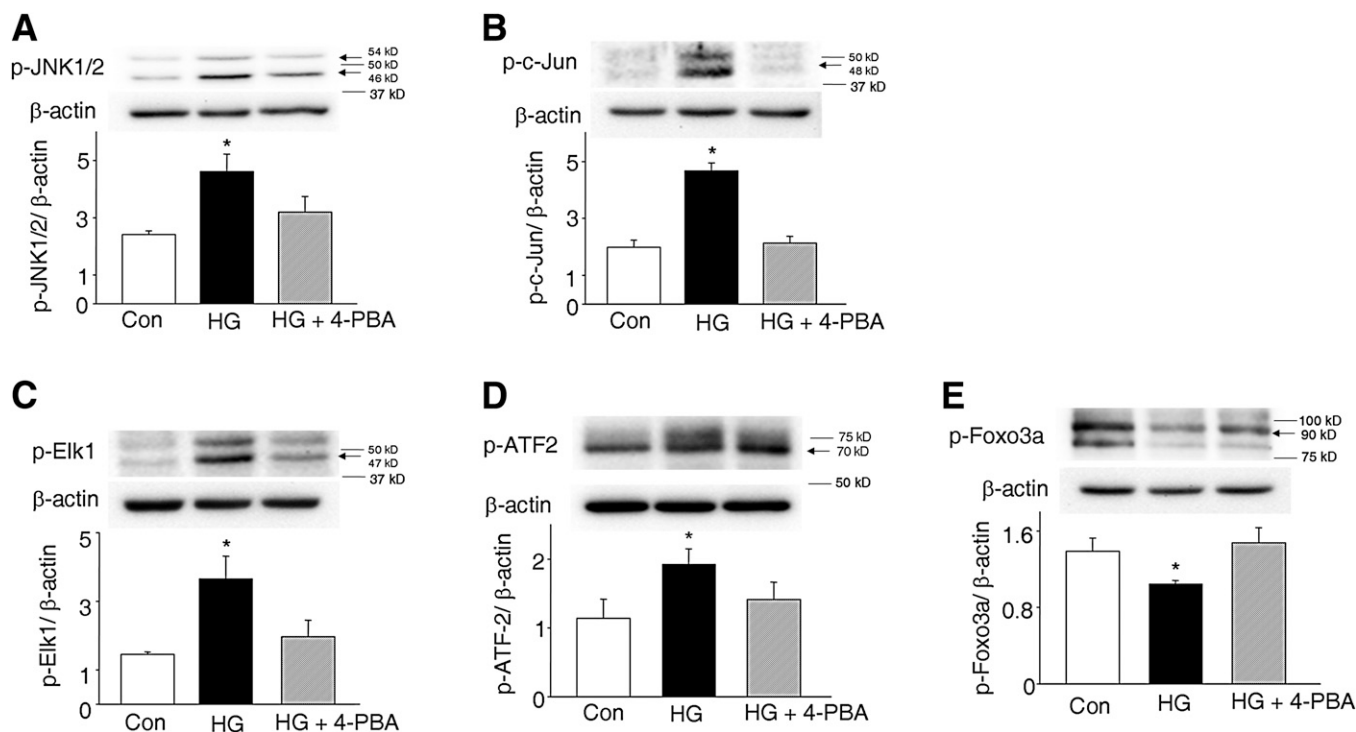


FIG. 6. 4-PBA treatment blocks high glucose–induced JNK1/2 pathway activation. Levels of p-JNK1/2 (A), p-c-Jun (B), p-Elk1 (C), p-ATF-2 (D), and p-Foxo3a (E) in embryos cultured under 5 mmol/L glucose (control [Con]), 20 mmol/L glucose (high glucose [HG]), and 20 mmol/L glucose plus 2 mmol/L 4-PBA conditions (HG + 4-PBA). Experiments were repeated three times using samples from three independent cultures. In A–E, arrows point to the actual sizes of the targeted proteins, and adjacent protein markers are indicated. *Significant difference ($P < 0.05$) compared with the other two groups.

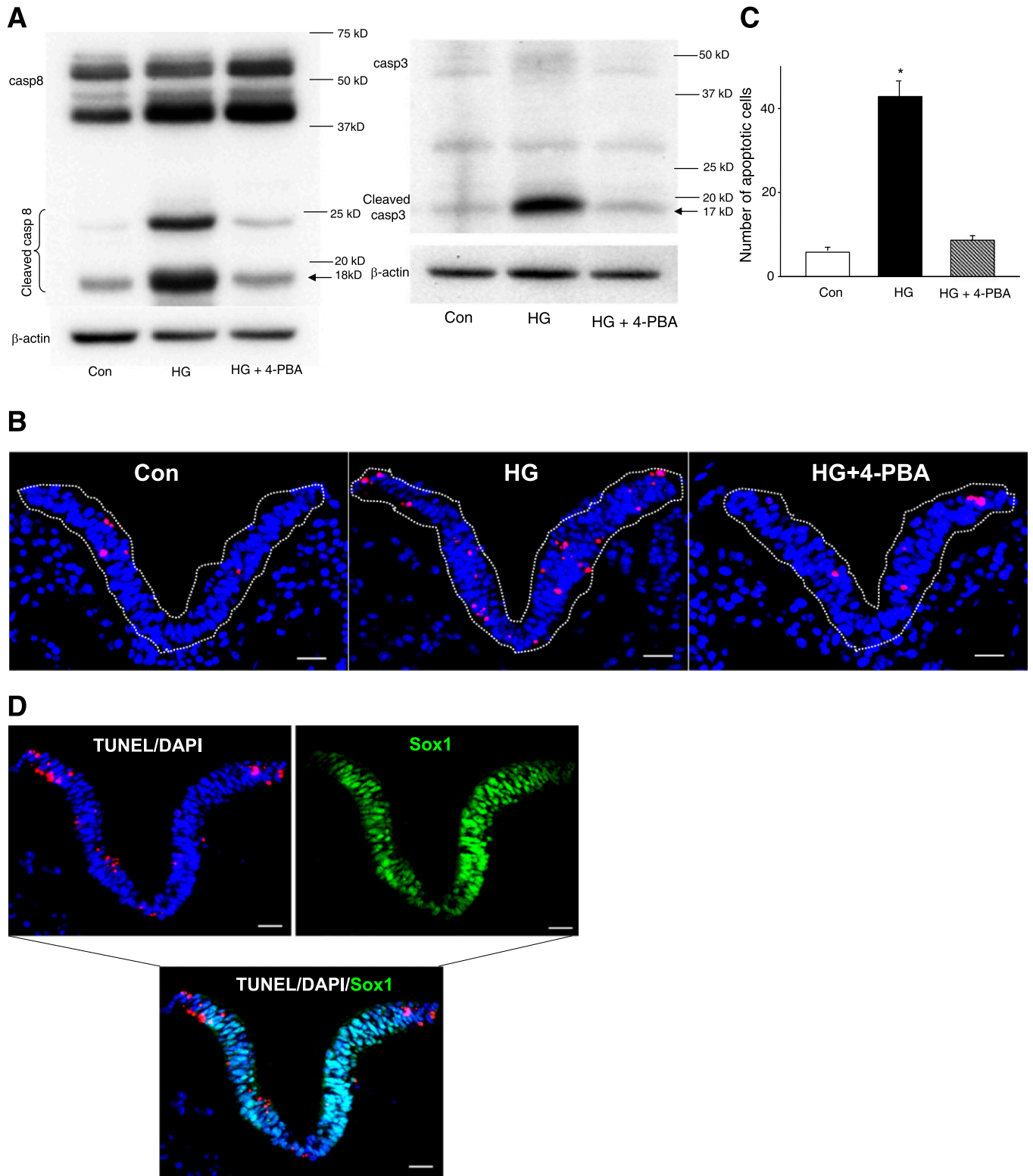


FIG. 7. 4-PBA treatment abolishes high glucose–induced caspase activation and neuroepithelial cell apoptosis. In *A*, cleaved caspase 3 and 8 were analyzed in embryos cultured under 5 mmol/L glucose (control [Con]), 20 mmol/L glucose (high glucose [HG]), and 20 mmol/L glucose plus 2 mmol/L 4-PBA conditions (HG + 4-PBA). Experiments were repeated three times using cultured embryos from different dams, and similar results for caspase cleavage were obtained. Representative images of the TUNEL assays are shown in *B*. Apoptotic cells are labeled in red, and all cells are labeled in blue. The dense blue areas, which are marked by white dash lines, are neuroepithelia of cultured embryos. Scale bars, 30 μ m. *C* shows quantification of apoptotic cells in the whole anterior neural tube of 12-h cultured embryos. Five serial coronal sections through the anterior neural tubes of each embryo were analyzed. In each group, six embryos from three independent cultures were used. The numbers of apoptotic cells were counted in the neural tube area of each section and averaged by the five sections for each embryo. In *D*, apoptotic cells labeled by TUNEL (red) staining are Sox1-positive (green) neural progenitors in the neuroepithelia of the HG group. The same section was sequentially stained by TUNEL, DAPI, and Sox1. Cell nuclei were stained by DAPI in blue. Scale bars, 30 μ m. *Significant difference ($P < 0.01$) compared with the other two groups. (A high-quality color representation of this figure is available in the online issue.)

Our study presents for the first time strong evidence that JNK1/2 activation leads to ER stress. In future studies, it will be of interest to delineate the mechanisms underlying JNK1/2-induced ER stress. Factors that disrupt ER function and thus induce ER stress include accumulation of protein aggregates, oxidative stress, and alterations in calcium stores in the ER lumen (34). Because JNK1/2 activation can directly increase reactive oxygen species production (39), JNK1/2 may trigger ER stress via oxidative stress. JNK1/2 activation also contributes to the formation of intracellular protein aggregates (40), which may result in ER stress. JNK1/2 activates Bid (41), a proapoptotic Bcl-2 family member, which controls ER calcium homeostasis (42). Therefore, it is possible that JNK1/2 induces ER stress by disrupting ER calcium homeostasis. The mechanisms underlying JNK1/2-induced ER stress are likely multifactorial.

JNK1^{+/-} and JNK2^{-/-} mice are viable, normal in size, do not display any gross physical or behavioral abnormalities, and display normal embryonic development (43). Indeed, embryos from either nondiabetic JNK1^{+/-} or nondiabetic JNK2^{-/-} dams are morphologically indistinct from those from nondiabetic WT mice (21,43,44). We have successfully established the causal link between JNK1/2 activation and ER stress by using *jnk2*^{-/-} and *jnk1*^{+/-} mice. Using a *jnk1*^{+/-} and *jnk1*^{+/-} mating scheme to produce JNK1-null embryos avoids any potential maternal influences due to gene deletion. However, any potential maternal influence due to *jnk2* gene deletion in diabetic embryopathy is negligible because diabetic JNK2KO dams have similar high glucose levels as those in diabetic WT mice (21). A recent published report (26) also used homozygous knockout mating in diabetes-induced NTD. Therefore, the JNK2 homozygous mating scheme is a suitable approach in our study.

Either *jnk1* or *jnk2* gene deletion blocks maternal diabetes-induced ER chaperone gene expression and consequent ER stress. Mitigating ER stress by 4-PBA treatment, in turn, blocks JNK1/2 activation, its downstream apoptotic signaling, and NTD. Our study establishes the reciprocal and interdependent link between the two causative events, JNK1/2 activation and ER stress, in diabetic embryopathy.

ACKNOWLEDGMENTS

This study is supported by National Institutes of Health grants R01-DK-083243 and R01-DK-083770.

No potential conflicts of interest relevant to this article were reported.

X.L. and C.X. researched data and approved the final version of the manuscript. P.Y. conceived the project, designed the experiments, researched data, and wrote and approved the final version of the manuscript. P.Y. is the guarantor of this work and, as such, had full access to all the data in the study and takes responsibility for the integrity of the data and the accuracy of the data analysis.

The authors thank Dr. E. Albert Reece at the University of Maryland School of Medicine for editing the manuscript and Ms. Hua Li at the University of Maryland School of Medicine for technical support.

REFERENCES

- Becerra JE, Khoury MJ, Cordero JF, Erickson JD. Diabetes mellitus during pregnancy and the risks for specific birth defects: a population-based case-control study. *Pediatrics* 1990;85:1-9
- Correa A, Gilboa SM, Besser LM, et al. Diabetes mellitus and birth defects. *Am J Obstet Gynecol* 2008;199:237.e1-9
- Yang X, Borg LA, Eriksson UJ. Altered metabolism and superoxide generation in neural tissue of rat embryos exposed to high glucose. *Am J Physiol* 1997;272:E173-E180
- Phelan SA, Ito M, Loeken MR. Neural tube defects in embryos of diabetic mice: role of the Pax-3 gene and apoptosis. *Diabetes* 1997;46:1189-1197
- Gäreskog M, Cederberg J, Eriksson UJ, Wentzel P. Maternal diabetes in vivo and high glucose concentration in vitro increases apoptosis in rat embryos. *Reprod Toxicol* 2007;23:63-74
- Yang P, Zhao Z, Reece EA. Activation of oxidative stress signaling that is implicated in apoptosis with a mouse model of diabetic embryopathy. *Am J Obstet Gynecol* 2008;198:130.e1-7
- Salbaum JM, Kappen C. Neural tube defect genes and maternal diabetes during pregnancy. *Birth Defects Res A Clin Mol Teratol* 2010;88:601-611
- Pavlinkova G, Salbaum JM, Kappen C. Maternal diabetes alters transcriptional programs in the developing embryo. *BMC Genomics* 2009;10:274
- Wentzel P, Gäreskog M, Eriksson UJ. Decreased cardiac glutathione peroxidase levels and enhanced mandibular apoptosis in malformed embryos of diabetic rats. *Diabetes* 2008;57:3344-3352
- Yang X, Borg LA, Eriksson UJ. Altered mitochondrial morphology of rat embryos in diabetic pregnancy. *Anat Rec* 1995;241:255-267
- Reece EA, Pinter E, Leranth CZ, et al. Ultrastructural analysis of malformations of the embryonic neural axis induced by in vitro hyperglycemic conditions. *Teratology* 1985;32:363-373
- Szegezdi E, Logue SE, Gorman AM, Samali A. Mediators of endoplasmic reticulum stress-induced apoptosis. *EMBO Rep* 2006;7:880-885
- Ron D, Walter P. Signal integration in the endoplasmic reticulum unfolded protein response. *Nat Rev Mol Cell Biol* 2007;8:519-529
- Ron D, Hubbard SR. How IRE1 reacts to ER stress. *Cell* 2008;132:24-26
- Harding HP, Zhang Y, Ron D. Protein translation and folding are coupled by an endoplasmic-reticulum-resident kinase. *Nature* 1999;397:271-274
- Lee K, Tirasophon W, Shen X, et al. IRE1-mediated unconventional mRNA splicing and S2P-mediated ATF6 cleavage merge to regulate XBP1 in signaling the unfolded protein response. *Genes Dev* 2002;16:452-466
- Zinszner H, Kuroda M, Wang X, et al. CHOP is implicated in programmed cell death in response to impaired function of the endoplasmic reticulum. *Genes Dev* 1998;12:982-995
- Reece EA, Ma XD, Zhao Z, Wu YK, Dhanasekaran D. Aberrant patterns of cellular communication in diabetes-induced embryopathy in rats: II, apoptotic pathways. *Am J Obstet Gynecol* 2005;192:967-972
- Forsberg H, Eriksson UJ, Welsh N. Apoptosis in embryos of diabetic rats. *Pharmacol Toxicol* 1998;83:104-111
- Sun F, Kawasaki E, Akazawa S, et al. Apoptosis and its pathway in early post-implantation embryos of diabetic rats. *Diabetes Res Clin Pract* 2005;67:110-118
- Yang P, Zhao Z, Reece EA. Involvement of c-Jun N-terminal kinases activation in diabetic embryopathy. *Biochem Biophys Res Commun* 2007;357:749-754
- Urano F, Wang X, Bertolotti A, et al. Coupling of stress in the ER to activation of JNK protein kinases by transmembrane protein kinase IRE1. *Science* 2000;287:664-666
- Hagay ZJ, Weiss Y, Zusman I, et al. Prevention of diabetes-associated embryopathy by overexpression of the free radical scavenger copper zinc superoxide dismutase in transgenic mouse embryos. *Am J Obstet Gynecol* 1995;173:1036-1041
- Yang P, Reece EA. Role of HIF-1alpha in maternal hyperglycemia-induced embryonic vasculopathy. *Am J Obstet Gynecol* 2011;204:332.e1-7
- Eriksson UJ, Dahlström E, Hellerström C. Diabetes in pregnancy. Skeletal malformations in the offspring of diabetic rats after intermittent withdrawal of insulin in early gestation. *Diabetes* 1983;32:1141-1145
- Sugimura Y, Murase T, Oyama K, et al. Prevention of neural tube defects by loss of function of inducible nitric oxide synthase in fetuses of a mouse model of streptozotocin-induced diabetes. *Diabetologia* 2009;52:962-971
- Kamimoto Y, Sugiyama T, Kihira T, et al. Transgenic mice overproducing human thioredoxin-1, an antioxidative and anti-apoptotic protein, prevents diabetic embryopathy. *Diabetologia* 2010;53:2046-2055
- Massa V, Savery D, Ybot-Gonzalez P, et al. Apoptosis is not required for mammalian neural tube closure. *Proc Natl Acad Sci USA* 2009;106:8233-8238
- Reece EA, Ji I, Wu YK, Zhao Z. Characterization of differential gene expression profiles in diabetic embryopathy using DNA microarray analysis. *Am J Obstet Gynecol* 2006;195:1075-1080
- Reece EA, Wu YK. Prevention of diabetic embryopathy in offspring of diabetic rats with use of a cocktail of deficient substrates and an antioxidant. *Am J Obstet Gynecol* 1997;176:790-797; discussion 797-798

31. Yang P, Zhao Z, Reece EA. Blockade of c-Jun N-terminal kinase activation abrogates hyperglycemia-induced yolk sac vasculopathy in vitro. *Am J Obstet Gynecol* 2008;198:321.e1-7
32. Yang P, Li H. Epigallocatechin-3-gallate ameliorates hyperglycemia-induced embryonic vasculopathy and malformation by inhibition of Foxo3a activation. *Am J Obstet Gynecol* 2010;203:75.e1-6
33. Ozcan U, Yilmaz E, Ozcan L, et al. Chemical chaperones reduce ER stress and restore glucose homeostasis in a mouse model of type 2 diabetes. *Science* 2006;313:1137-1140
34. Tabas I, Ron D. Integrating the mechanisms of apoptosis induced by endoplasmic reticulum stress. *Nat Cell Biol* 2011;13:184-190
35. Kim HR, Lee GH, Cho EY, Chae SW, Ahn T, Chae HJ. Bax inhibitor 1 regulates ER-stress-induced ROS accumulation through the regulation of cytochrome P450 2E1. *J Cell Sci* 2009;122:1126-1133
36. Naderi J, Hung M, Pandey S. Oxidative stress-induced apoptosis in dividing fibroblasts involves activation of p38 MAP kinase and over-expression of Bax: resistance of quiescent cells to oxidative stress. *Apoptosis* 2003;8:91-100
37. Pugazhenth S, Nesterova A, Jambal P, et al. Oxidative stress-mediated down-regulation of bcl-2 promoter in hippocampal neurons. *J Neurochem* 2003;84:982-996
38. Gäreskog M, Eriksson UJ, Wentzel P. Combined supplementation of folic acid and vitamin E diminishes diabetes-induced embryotoxicity in rats. *Birth Defects Res A Clin Mol Teratol* 2006;76:483-490
39. Ventura JJ, Cogswell P, Flavell RA, Baldwin AS Jr, Davis RJ. JNK potentiates TNF-stimulated necrosis by increasing the production of cytotoxic reactive oxygen species. *Genes Dev* 2004;18:2905-2915
40. Cowan KJ, Diamond MI, Welch WJ. Polyglutamine protein aggregation and toxicity are linked to the cellular stress response. *Hum Mol Genet* 2003;12:1377-1391
41. Deng Y, Ren X, Yang L, Lin Y, Wu X. A JNK-dependent pathway is required for TNFalpha-induced apoptosis. *Cell* 2003;115:61-70
42. Ni HM, Baty CJ, Li N, et al. Bid agonist regulates murine hepatocyte proliferation by controlling endoplasmic reticulum calcium homeostasis. *Hepatology* 2010;52:338-348
43. Kuan CY, Yang DD, Samanta Roy DR, Davis RJ, Rakic P, Flavell RA. The Jnk1 and Jnk2 protein kinases are required for regional specific apoptosis during early brain development. *Neuron* 1999;22:667-676
44. Li X, Weng H, Xu C, Reece EA, Yang P. Oxidative stress-induced JNK1/2 activation triggers pro-apoptotic signaling and apoptosis that leads to diabetic embryopathy. *Diabetes* 2012;61:2084-2092